A newly developed anesthetic based on a unique chemical core

Noëlie S. Cayla[a], Beza A. Dagne[a], Yun Wu[a], Yao Lu[a], Larry Rodriguez[b], Daryl L. Davies[b], Eric R. Gross[a], Boris D. Heifets[a], M. Frances Davies[a,c], M. Bruce MacIver[a], and Edward J. Bertaccini[a,c,1]

[a]Department of Anesthesiology, Perioperative and Pain Medicine, Stanford University School of Medicine, Stanford, CA 94305; [b]Department of Molecular Pharmacology and Toxicology, University of Southern California School of Pharmacy, Los Angeles, CA 90089; and [c]Department of Anesthesia, Palo Alto VA Health Care System, Palo Alto, CA 94304

Edited by Emery N. Brown, Massachusetts General Hospital, Boston, MA, and approved June 19, 2019 (received for review December 28, 2018)

Intravenous anesthetic agents are associated with cardiovascular instability and poorly tolerated in patients with cardiovascular disease, trauma, or acute systemic illness. We hypothesized that a new class of intravenous (IV) anesthetic molecules that is highly selective for the slow type of γ-aminobutyric acid type A receptor ($GABA_AR$) could have potent anesthetic efficacy with limited cardiovascular effects. Through in silico screening using our $GABA_AR$ model, we identified a class of lead compounds that are *N*-arylpyrrole derivatives. Electrophysiological analyses using both an in vitro expression system and intact rodent hippocampal brain slice recordings demonstrate a $GABA_AR$-mediated mechanism. In vivo experiments also demonstrate overt anesthetic activity in both tadpoles and rats with a potency slightly greater than that of propofol. Unlike the clinically approved GABAergic anesthetic etomidate, the chemical structure of our *N*-arylpyrrole derivative is devoid of the chemical moieties producing adrenal suppression. Our class of compounds also shows minimal to no suppression of blood pressure, in marked contrast to the hemodynamic effects of propofol. These compounds are derived from chemical structures not previously associated with anesthesia and demonstrate that selective targeting of $GABA_AR$-slow subtypes may eliminate the hemodynamic side effects associated with conventional IV anesthetics.

anesthesia | drug discovery | mechanism | gamma amino butyric acid receptor

Anesthetics have been successfully administered for over 170 y. Unfortunately, all current IV anesthetic agents have detrimental side effects, most notably hemodynamic suppression. It is for this reason that we have ventured to design a class of anesthetics that are devoid of such side effects. Our drug design strategy has been based on the recent advances in computational chemistry which lead to a validated model of the gamma amino butyric acid type A receptor $GABA_AR$ (1, 2). Sophisticated molecular computations, previously only available via supercomputing facilities, can now be achieved with advanced desktop workstations. Software development has taken full advantage of high-end 3D visualization as well as highly parallelized computational algorithms for efficient drug screening methodologies. Along with these advances, our understanding of the molecular substrates for conscious states has also progressed in the form of robust models of a $GABA_AR$ ligand-gated ion channel that is known to mediate important anesthetic actions (3). The concept presented here is to leverage such advances in computational capabilities for high throughput in silico screening to perform efficient lead compound refinement and drug design using our newly developed molecular models of the $GABA_AR$. Our current work has now identified a class of lead compounds that demonstrate overt anesthetic activity in mammals via a $GABA_AR$ mechanism, while producing minimal to no hemodynamic perturbations. This is a marked improvement over the detrimental effects of propofol on blood pressure, the current gold standard of IV anesthetics.

After modeling the unwanted interaction of etomidate with the enzyme 11-β-hydroxylase, believed to cause adrenal suppression (4, 5) we investigated alternatives suggested by previous findings (6–9), and then designed a unique molecular core in silico. A selection of 11 lead compounds were identified as similar to our newly designed core after high-throughput structural screening. Subsequent molecular docking was performed using our current $GABA_AR$ model. These compounds were then tested on acutely dissected rodent brain slices and *Xenopus* oocytes for validation of $GABA_AR$-mediated inhibition mechanisms and in vivo in tadpoles for loss-of-righting reflex (LORR). The most potent compound of the series (BB) was then tested for both LORR and hemodynamic effects in rats.

Results

Molecular Modeling of the 11-β-Hydroxylase Enzyme and Its Interactions with Etomidate, Carboetomidate, 1n, and Carbo-1n. Anesthetics interact with many functional proteins, resulting in a variety of important side effects. In particular, etomidate has a strong inhibitory effect on a critical enzyme for steroid biosynthesis, 11-beta-hydroxylase (11CYPB). This effect can result in considerable adrenocortical suppression. A deeper understanding of this process requires a more thorough molecular description of the relevant drug–protein

Significance

The 4 intravenous anesthetics currently in clinical use are associated with undesirable side effects such as lower blood pressure. These agents are poorly tolerated in young and elderly patients, limiting their use and increasing their risks. Additionally, etomidate, an anesthetic that achieves stable cardiovascular conditions, causes significant adrenal suppression by inhibiting steroid biosynthesis. Even though the exact mechanisms of anesthesia remain unknown, a significant component appears to be mediated by γ-aminobutyric acid type A receptors ($GABA_ARs$). By targeting an anesthetic binding site in these receptors, we are designing anesthetics with reduced side effects. A unique agent based on this design is now shown to be potent and selective for $GABA_A$-slow receptors and produces anesthesia with minimal hemodynamic side effects.

Author contributions: D.L.D., E.R.G., B.D.H., M.B.M., and E.J.B. designed research; N.S.C., B.A.D., Y.W., Y.L., L.R., D.L.D., E.R.G., B.D.H., M.F.D., and E.J.B. performed research; E.J.B. contributed new reagents/analytic tools; N.S.C., L.R., B.D.H., M.F.D., and E.J.B. analyzed data; and N.S.C., L.R., B.D.H., M.F.D., M.B.M., and E.J.B. wrote the paper.

Conflict of interest statement: E.J.B. and M.F.D. are coinventors on the patent WO 2016/061538 A1 "Novel Methods, Compounds, and Compositions for Anesthesia" and they, their department, and their institution could receive royalties related to the development of these new anesthetic agents.

This article is a PNAS Direct Submission.

[1]To whom correspondence may be addressed. Email: edwardb@stanford.edu.

This article contains supporting information online at www.pnas.org/lookup/suppl/doi:10.1073/pnas.1822076116/-/DCSupplemental.

Published online July 15, 2019.

interactions. While the exact molecular structure of all forms of 11CYPB remain unknown, significant progress has been made toward understanding their interactions with anesthetics using molecular modeling as noted here. We therefore built a molecular model of 11CYPB and performed in silico docking analyses of several important ligands to its binding site. The basic local alignment search tool (BLAST) derived scores and CLUSTALW profile-to-profile alignment demonstrated reasonable sequence similarity between 11CYPB and the modeling templates. The model of the 11CYPB has a cavity of ~810 Å^3 and can readily accommodate a steroid analog. Within the lowest frequency, highest amplitude natural harmonic motions of this channel, normal mode analyses suggest that this cavity is located in a region of reasonable flexibility, which could be critical to a "clamshell-like" opening motion for binding site access. Etomidate, carboetomidate, 1n, and carbo-1n docking reveal a potentially reversible carbonyl interaction with the heme iron; however, only etomidate and 1n clearly show an imidazole nitrogen available for strong coordinate bond interaction with the heme iron (*SI Appendix*, Fig. S1). Therefore, it is predicted that carbo-1n and its relatives derived from the similarity search of the Chemical Abstracts database should not significantly inhibit steroid biosynthesis. This result is consistent with the already experimentally derived validation of the loss of adrenal suppression via the lack of 11CYPB suppression shown by Raines et al. with their conversion of an imidazole to a pyrrole in the making of carboetomidate (9).

In Silico Modeling and High-Throughput Screening Lead to a Selection of Compounds Whose Relative Potencies Are Predicted via Molecular Docking to the GABA$_A$R. In our previous work, docking of the initial propofol derivative series to the region bound by specific anesthetic binding residues showed strong linear correlation with the experimentally derived EC_{50} for GABA$_A$R potentiation as suggested by an R^2 of 0.85 (1, 2). CDocker scoring was also validated by the results of the control compounds with known inactivity at the GABA$_A$R. In the current work (Fig. 1), additional docking of the members from the substituted 1,2-diphenylimidazole series from Asproni et al. (6) which includes 1n (also known as TG41 in their other work) showed a strong correlation of a slightly different docking score, the CDocker Interaction Energy (CDIE) score, with experimentally derived GABA$_A$R potentiation EC_{50}. This correlation not only spanned the previously studied propofol-like compounds, but included several of the etomidate-like derivatives, as well as carbo-1n, in addition to the 11 compounds similar to carbo-1n. In particular, one experimental compound, BB, appears to be about an order of magnitude less potent than 1n or TG41 which has a known EC_{50} for GABA$_A$R potentiation of 0.19 μM. However, the actual approximate EC_{50} for GABA$_A$R potentiation of BB appears to be around 0.5 μM in both patch clamp studies as well as tadpoles as noted below.

LORR Assays Confirm Anesthetic Activity and Determine a Lead Compound. Seven of the 11 compounds in Fig. 2 that were tested for LORR in tadpoles had potencies less than 40 μM (Fig. 3*A*). Compounds AA and BB showed potent anesthetic activities as predicted by the in silico modeling. The EC_{50} measurements in the tadpoles (Fig. 3 *B* and *C*) showed that BB was more potent than AA (0.49 μM for BB, and 1.5 μM for AA). The slope of the BB dose–response curves were very steep. All tadpoles recovered a robust LORR once placed into a water bath without drug. After this second round of screening, BB was chosen as the lead compound. Its anesthetic activity was subsequently tested in rats via LORR assays. Intravenous injection of the vehicle controls alone did not produce any behavioral effects. The ED_{50} value for this compound in rats was determined to be 4.3 mg/kg

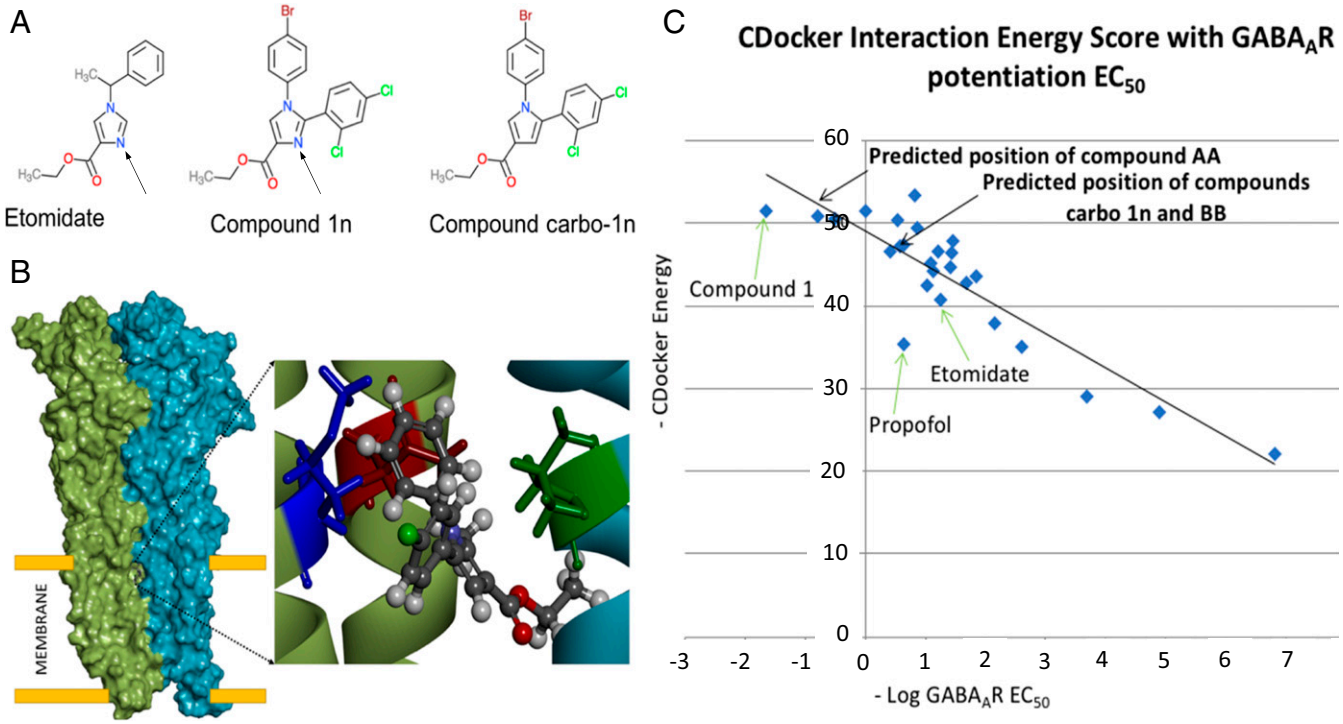

Fig. 1. In *A*, the arrow points to the nitrogen atom of etomidate involved in complexing with the heme iron in the enzyme, 11-β-hydroxylase, thereby inhibiting corticosteroid biosynthesis. A class of IV anesthetic was developed using a chemical core by converting the free nitrogen in the imidazole ring of 1n to a pyrrole ring shown in carbo-1n. The molecular model (*B*) shows an anesthetic binding site within the transmembrane component of the GABA$_A$R and the computationally docked structure of carbo-1n. *C* shows the docking scores of multiple compounds from the series involving 1n, propofol, and etomidate. These served as reference agents to approximate the GABA$_A$R docking scores of carbo-1n and its derivatives, notably AA and BB (see Fig. 2 for their structures). Their predicted positions noted by arrows predicted a potency making them worthy of subsequent experimental evaluation.

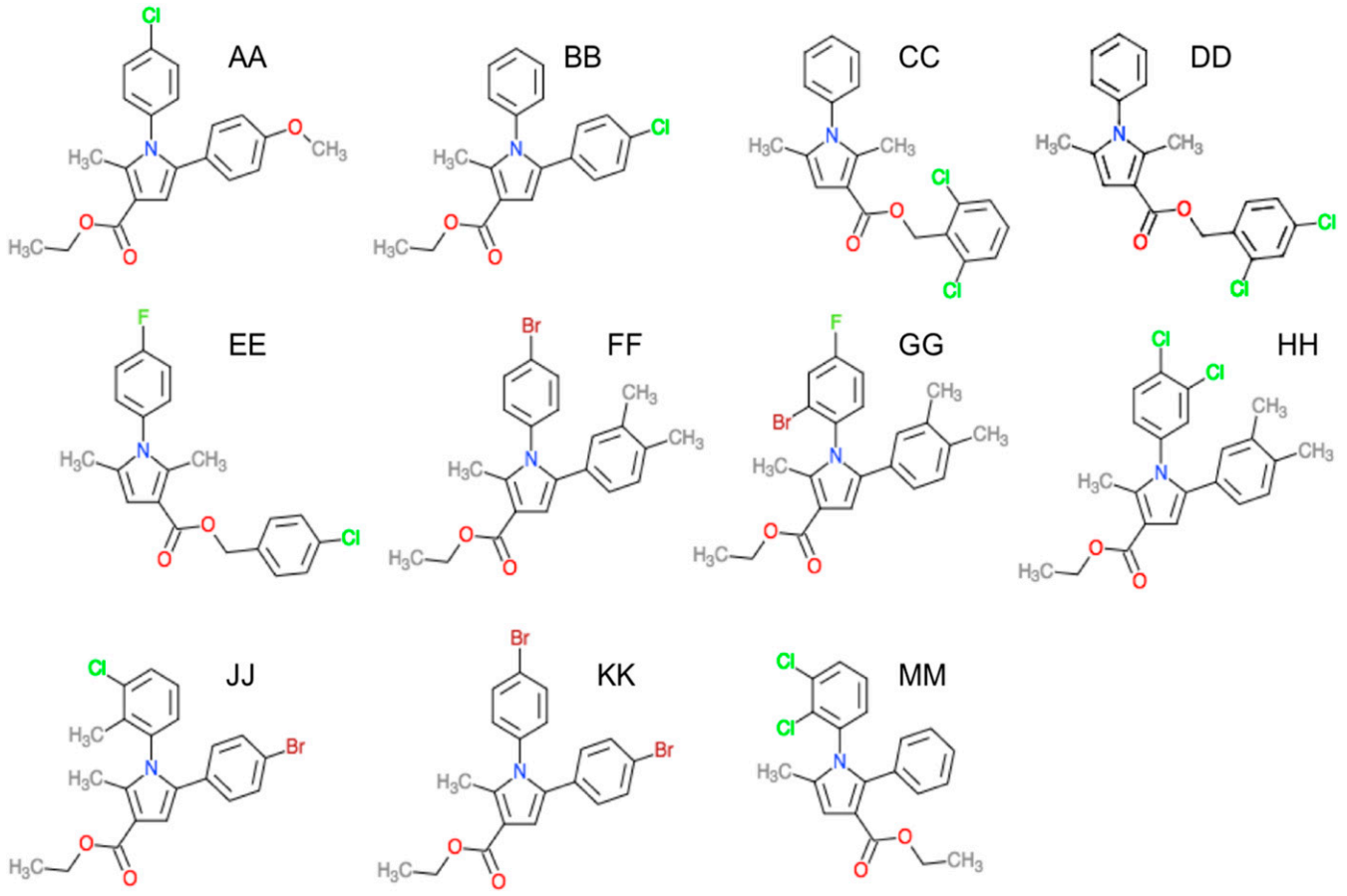

Fig. 2. Structures of the 11 compounds derived from the in silico structural similarity search for compounds resembling carbo-1n since the latter did not exist.

(95% confidence limits 3.9 to 4.7). Rodents ($n = 4$) injected with 8 mg/kg BB lost their righting reflex (nearly twice ED_{50}) at an average time of 2.0 ± 0.41 min and then recovered after an average time of 32 ± 1.9 min. They showed neither grossly abnormal behavioral effects nor any signs of toxicity.

Electrophysiology Recordings Show Evidence of $GABA_AR$-Mediated Inhibition. Acute hippocampal brain slices preserve major elements of synaptic and circuit organization observed in vivo while allowing for detailed electrophysiological investigation (10). We performed field recordings in the CA1 region, measuring population spikes evoked by paired electrical stimuli of afferents in the stratum radiatum, where the timing between the first and second pulse (100 ms) is optimized to test effects on $GABA_AR$-slow-mediated inhibition, as opposed to effects on $GABA_AR$-fast-mediated inhibition, measured using the first stimulus. The results shown in Fig. 4 demonstrate that etomidate and BB acted specifically through $GABA_AR$-slow receptors, since only the second pulse responses were depressed in experiments of paired-pulse inhibition. Propofol had additional effects mediated by $GABA_AR$-fast and tonic receptors (11, 12), since effects on both first and second pulse responses were produced (13). The effects of all agents were fully reversed by picrotoxin, a chloride channel blocker that acts specifically on $GABA_ARs$ (*SI Appendix*, Fig. S2). These results confirmed that BB produced a reversible enhancement of $GABA_AR$-slow-mediated inhibition, which was significantly more selective than propofol. The latter, in contrast, clearly enhanced other forms of $GABA_AR$-mediated inhibition by depressing both first and second pulse responses. Additionally, there was no effect of flumazenil on the BB response.

To directly measure BB's effect on $GABA_AR$-mediated currents in an intact tissue preparation, we performed whole-cell voltage-clamp recording from CA1 pyramidal cells in mice. Inhibitory postsynaptic currents (IPSCs) were pharmacologically isolated by the continuous perfusion of artificial cerebrospinal fluid (ACSF) containing NMDA and AMPA/Kainate receptor antagonists (25 μM d-APV and 10 μM NBQX), such that the resulting evoked current was entirely $GABA_AR$ mediated. GABA release and subsequent IPSCs were evoked by electrically stimulating afferent fibers in the stratum radiatum of the CA1 region, and IPSCs were recorded in the CA1 stratum pyramidale (Fig. 5*A*). This stimulation protocol is known to preferentially activate $GABA_AR$-slow inhibitory synapses (14). Decay constants and amplitude of the evoked IPSCs were monitored over time (Fig. 5 *B–D*), in addition to standard measures of whole-cell recording quality, i.e., series and input resistance (Fig. 5 *E* and *F*). A brief, 10-min perfusion of 40 μM BB dramatically slowed the decay of evoked IPSCs and produced a modest enhancement of IPSC amplitude. Notably, the vehicle did not have any effect on these measures. Changes in the quality of the pipette seal or changes in the cellular input resistance could not account for the observed slowing of IPSCs with BB (Fig. 5 *E* and *F*). The IPSC prolongation was substantial enough that currents which typically decayed to baseline in less than 50 ms extended to 100's of milliseconds in the presence of BB. The relatively selective effect on IPSC decay, versus amplitude, mirrors our finding that population spike pairs elicited at a 100-ms interval predominantly demonstrated a reduced second spike amplitude, without a notable effect on the first population spike amplitude.

A

Compound	EC_{50} (uM) for LORR
AA	1.5
BB	0.49
CC	~5
DD	~20
EE	~40
FF	~20
GG	3
HH	>40
JJ	>40
KK	~40
MM	~20

B

C

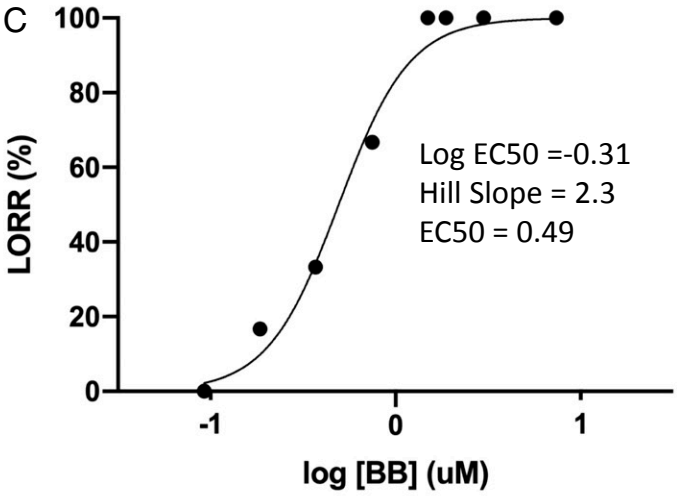

Fig. 3. The EC_{50} concentration for LORR for each compound (*A*) in bullfrog tadpoles (*B*) narrowed down the selection of 11 molecules suggested during the high-throughput screening stage to 1 lead compound. The most potent compound appeared to be BB (EC_{50} = 0.49 μM) (*C*) which was chosen for the rest of the experiments.

To allow a more detailed view of effects on $GABA_AR$-mediated currents, we tested BB on alpha5 containing $GABA_ARs$ expressed in *Xenopus* oocytes. Alpha5 containing $GABA_ARs$ is known to contribute to both $GABA_AR$-slow and tonic currents in CA1 pyramidal neurons (14–16). Fig. 6 illustrates the GABA concentration response curve for α5β3γ2 $GABA_ARs$ and demonstrated an EC_{50} of 6.6 ± 0.7 μM and EC_{20} of 3.2 ± 0.3 μM (Fig. 6*A*). BB robustly potentiated GABA-induced currents in a concentration-dependent manner, with an EC_{50} for GABA EC_{20} current potentiation of 0.57 ± 0.17 μM, very similar to the EC_{50} for the LORR in tadpoles (Fig. 6*B*).

In Vivo Hemodynamic Measures Demonstrate a Stable Cardiovascular Profile. The hemodynamic profiles for both BB and propofol were measured in rats and compared in Fig. 7. The ED_{50} dose of BB for LORR was 4.34 mg/kg (Fig. 7*A*). This is in comparison with the published ED_{50} for propofol of 5.13 mg/kg (17). Propofol readily produces a 50 ± 20% decrease in systolic (Fig. 7*B*) and diastolic (Fig. 7*D*) arterial blood pressure after a single IV bolus of 10.0 mg/kg (a typical anesthetic induction dose), while with BB, the values remain stable even at 20 mg/kg, a dose which is over 4× the ED_{50} required for LORR. Heart rate was not sensitive to either drug (Fig. 7*C*).

In Vivo Corticosteroid Assays Demonstrate a Stable Adrenal Profile. In silico calculations for our compounds predicted the lack of interaction with the heme iron in 11-β-hydroxylase and therefore an inability to suppress adrenal synthesis. This was experimentally tested by determining the effects of BB on corticosterone levels stimulated with $ACTH_{1–24}$ (0.5 mg/kg IV). The baseline levels of corticosterone before any drug was given were similar in both control vehicle and BB groups. After stimulation with ACTH and administration of either vehicle or BB, there was no difference in the stimulated corticosterone levels between control animals and those receiving BB (Fig. 8*A*), as well as no difference between groups in the change of stimulated corticosterone levels from baseline (Fig. 8*B*). Animals receiving either vehicle or BB both produced a marked increase in stimulated corticosterone levels from baseline (P = 0.0001, Fig. 8*A*) in response to ACTH. It should be noted that using the same protocol Wang et al. (18) found that etomidate caused an almost complete suppression of corticosterone synthesis.

Discussion

The drug profiles and dangerous side effects of the currently available IV anesthetic agents are many, especially among infants and the aging geriatric population. Proportionately, the fastest growing segment of the population are octogenarians and older, a group of people who now use the majority of the healthcare dollars and are in need of increasing surgical and anesthetic care. Even among an otherwise healthy population, conditions can arise that render any patient acutely unstable, such as in trauma and battlefield arenas. Therefore, there is significant clinical pressure as well as market opportunity to develop new anesthetics.

There are currently 4 main IV and 3 primary inhalational anesthetic agents in common clinical use. Each of these agents is associated with an entire spectrum of undesirable side effects, most of which result in lower systemic blood pressure (19). This side effect is poorly tolerated in very young children who possess immature cardiovascular compensatory mechanisms, as well as in the elderly with confounding comorbidities and otherwise

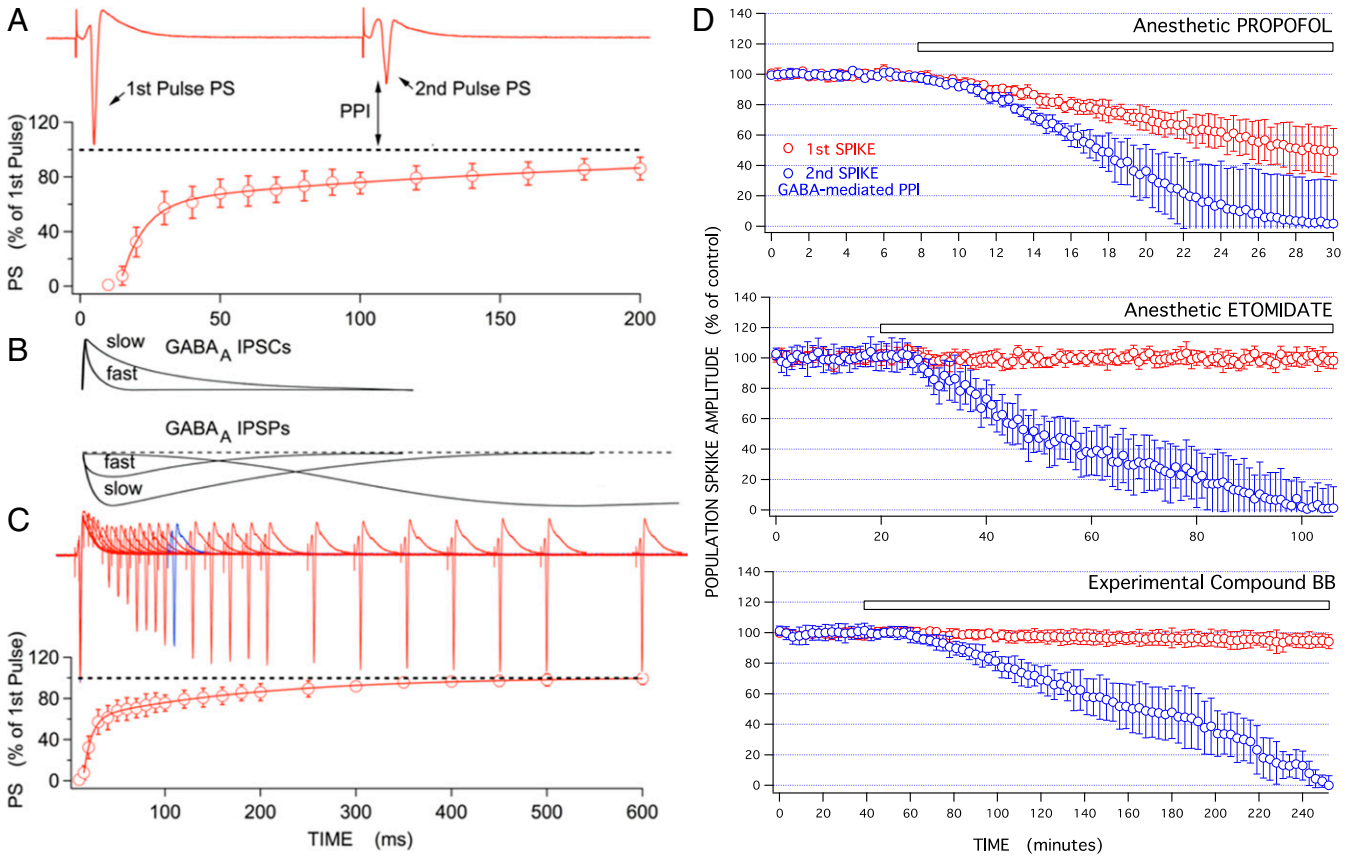

Fig. 4. (*A*) Paired-pulse population spike responses were recorded from hippocampal rat brain slices to measure anesthetic effects on tonic currents. Each symbol represents the mean ± SD for $n = 5$. (*B* and *C*) Fast (first pulse) and slow (second pulse) inhibitory pathways in the CA1 area neural circuit. By 100 ms it is too late to have the involvement of fast synapses, but ideal for following the time course of slow synapses. Each symbol represents the mean ± SD for $n = 5$ in *C*. Increased stimulation engages inhibitory circuitry, resulting in the paired pulse inhibition (PPI) measure between the first and second population spikes (PSs). Effects on tonic inhibition would contribute equally to both responses. (*D*) Population spike depression time course produced by propofol, etomidate, and BB showed significant differences in $GABA_AR$ involvement for first (in red) vs. second pulse responses (in blue). Minutes (min) are post-drug application. Each symbol represents the mean ± SD for $n = 10$ propofol; $n = 5$ etomidate; $n = 7$ BB. In *D*, the following statistical comparisons were made: first pulse propofol (30 min) vs. first pulse etomidate (40 min) $P < 0.005$; first pulse propofol (30 min) vs. first pulse BB (120 min) $P < 0.001$. For second pulse responses there were no significant differences between drugs for the depressions produced, since all produced 100% depression.

exhausted compensatory mechanisms. Each of these agents has additional unique detriments. In particular, etomidate is the agent which comes closest to achieving ideal cardiovascular preservation while inducing dose-dependent alterations in consciousness. However, this stability comes at the expense of clinically significant adrenal suppression via inhibited steroid biosynthesis. Propofol has gained wide popularity, but produces profound hypotension and, most notably in the very young, has also been associated with the propofol infusion syndrome characterized by extreme metabolic acidosis and death.

Several groups have developed compounds with similar overall shape to our lead class and that have effects at the $GABA_AR$. However, each has marked variation in their individual atomic constituents that not only make them chemically distinct, but are also characterized by variable physicochemical properties and methods of syntheses. For instance, the aryl pyrazoles described by Mascia et al. have a 5-membered ring at their core in which are adjacent nitrogens, variable halogen substitutions on the attached phenyl rings, and an amide-linked substituent (20). This is a class that is similar to many known cannabinoid receptor antagonists, which is also discussed in their work. The imidazole series presented by Asproni et al., while initially developed for other purposes, demonstrated several compounds with potent $GABA_AR$ activity (6). However, as alluded to above, they contain a central 5-membered imidazole ring, with variable attached phenyl ring substitutions and an ester group also with variable substitutions. Further, both the pyrazoles and the imidazoles contain a nitrogen with a free electron pair, making them susceptible to interaction with the heme iron of 11CYPB, therefore having the potential to produce adrenal suppression like etomidate.

In this study, we implemented state-of-the-art molecular computations, previously only available via supercomputing facilities that combine advanced molecular modeling and 3D visualization with highly parallelized computational algorithms for efficient drug screening in an effort to design the next generation of safer IV anesthetic. We iteratively leveraged this technology to identify leads based on our validated models of the anesthetic binding site within the $GABA_AR$ for subsequent in vitro and in vivo measures of potency and physiologic effects. A successful computational selection of 11 potential anesthetic agents with the desired pharmacologic characteristics allowed the identification of a lead compound, BB, with a safer and more potent profile exhibited during in vitro and in vivo studies of anesthetic efficacy. The concept presented here demonstrates the advantages of high-throughput in silico screening (via structural screening and ligand-receptor docking methodologies) in an effort to better perform efficient lead refinement and drug design using current molecular models of the $GABA_AR$. Mechanistically, a class of anesthetic compounds has been identified that is devoid of the moiety known to produce adrenal suppression in etomidate.

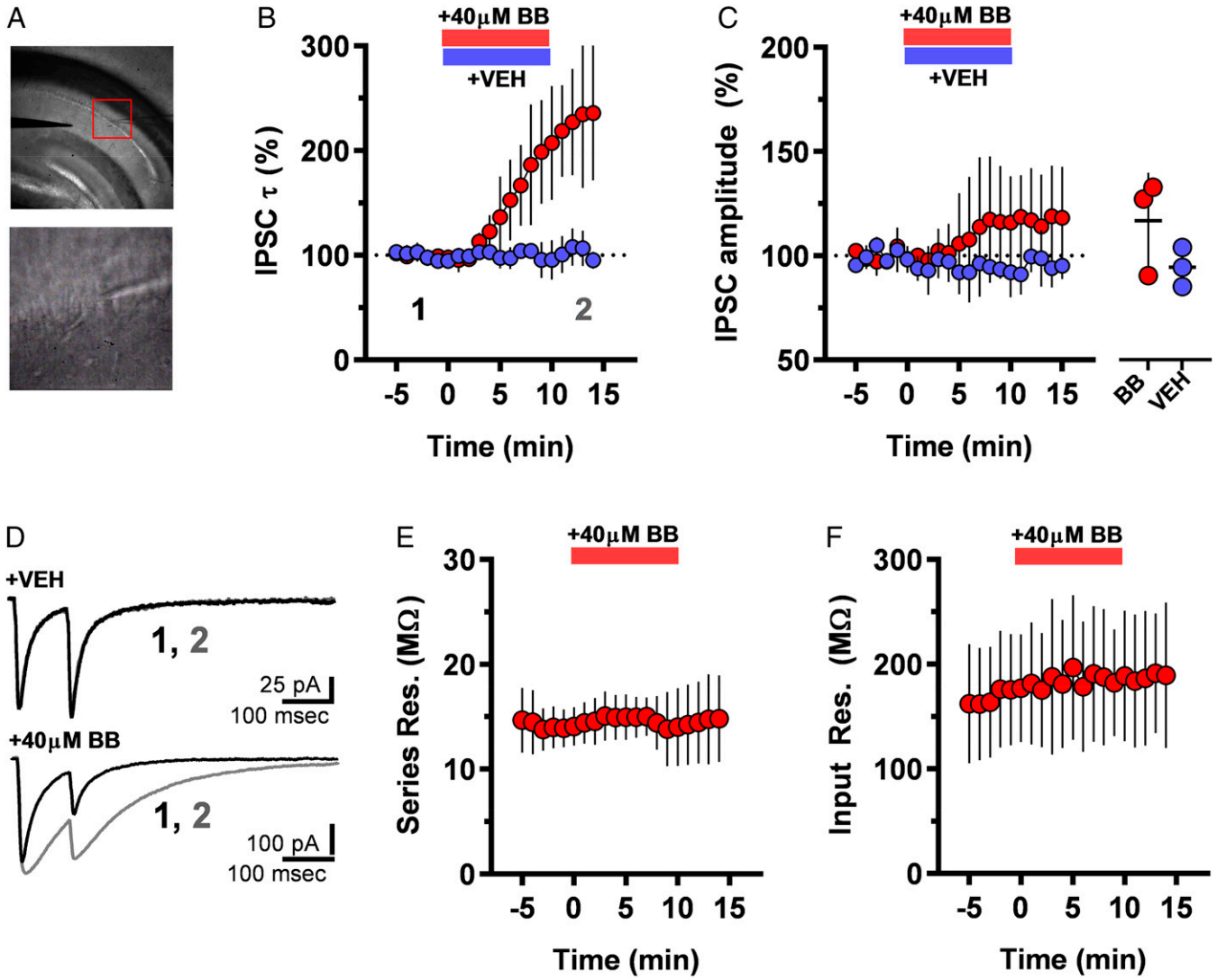

Fig. 5. Compound BB dramatically prolongs $GABA_AR$-mediated IPSCs. (*A*) Configuration for electrically evoking and recording IPSCs. (*A*, *Top*) Photomicrograph (10×) of a transverse hippocampal slice from mouse. Monopolar stainless steel stimulating electrode is placed in the stratum radiatum, and recording pipette in the stratum pyramidale, of hippocampal area CA1. Red box indicates field of magnified image (60×) at *Bottom*, in which the recording pipette is attached to a pyramidal cell. (*B*) IPSC duration, measured by the monoexponential decay constant, τ, is significantly prolonged in the presence of BB, but not vehicle (VEH). VEH or 40 μM BB compound was perfused into the recording chamber from time 0 until time 10. Points 1 and 2 indicate times where representative evoked IPSC traces (*D*) were taken. At *Right* of graph, the % change of τ versus predrug baseline is shown for both BB and VEH conditions. Individual cell data and group mean ± SD are plotted for the epoch between 10 and 15 min after BB/VEH application. (*C*) In the same set of experiments shown in *B*, BB, but not VEH, modestly enhanced IPSC amplitude. Changes of IPSC amplitude versus baseline are again shown at *Right* of graph for individual cells and group mean ± SD. (*D*) Representative IPSC traces before and after application of VEH or BB (time points indicated in *B*). (*E* and *F*) BB did not change parameter recording quality, as measured by resistance of the recording electrode in series with the recorded cell (series resistance, *E*) and the cell's global resistance to alterations in membrane potential (input resistance, *F*), indicating little or no effect on tonic $GABA_AR$ currents were produced.

Subsequent experiments were thereby made more efficient and limited in scope to confirm its anesthetic efficacy in mammals.

It was particularly interesting that BB exhibited a selective depression of the second pulse of a pair of stimuli used to test for effects on $GABA_AR$-slow IPSCs, since $GABA_AR$-fast responses decay long before the 100-ms interval used for the second test pulse. BB shared this selective effect with etomidate, but not with propofol. Propofol depressed both first and second pulse responses, indicating direct effects on both $GABA_AR$-fast and -slow forms of inhibition, as well as tonic $GABA_ARs$ that contribute to the first pulse depression observed (12). Propofol shares this first pulse depression with volatile anesthetics and barbiturates that also produce hemodynamic and respiratory depression (11). This suggests that nonselective actions on tonic and fast $GABA_ARs$ could contribute to the unwanted hemodynamic side effects, while the common action of enhanced $GABA_AR$-slow inhibition is needed for anesthesia.

In conclusion, our methodologies of in silico screening and prediction of compounds that bind to our validated model of the $GABA_AR$ have now identified a class of lead compounds that demonstrate overt anesthetic activity in both tadpoles and rats with a potency greater than that of propofol, the current IV anesthetic standard. These structures are devoid of the chemical moieties known to produce adrenal suppression, a serious side effect of the other commonly used anesthetic, etomidate. Of even greater importance is the fact that BB, the lead representative of this class of compounds, shows minimal to no suppression of blood pressure, in stark contrast to the deleterious hemodynamic

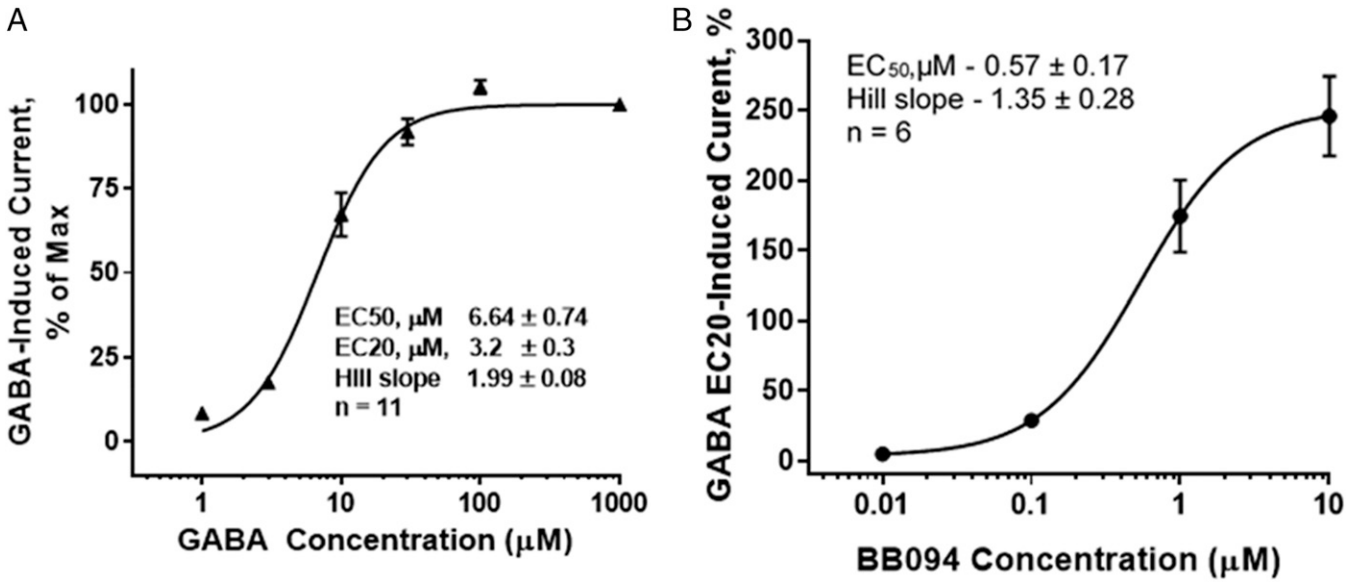

Fig. 6. Whole-cell oocyte voltage-clamp recordings lead to the above dose–response curves. *A* illustrates the GABA concentration response curve for $\alpha5\beta3\gamma2$ $GABA_AR$s that demonstrated an EC_{50} of 6.6 μM and EC_{20} of 3.2 μM. *B* shows the BB concentration-response curve in the presence of GABA EC_{20}-induced currents for alpha5 $GABA_AR$ ($\alpha5\beta3\gamma2$). Error bars refer to SEs from the mean.

effects of propofol. Several forms of electrophysiologic analyses from both ion channel patch clamp studies as well as in vitro rat hippocampal brain slice recordings are consistent with a selective targeting of $GABA_A$ receptor subtypes.

Methods

All experimental protocols involving either rodents or tadpoles were approved by the Administrative Panel on Laboratory Animal Care (APLAC) from Stanford University and the Institutional Animal Care and Use Committee (IACUC) from the Palo Alto VA Health Care System.

In Silico Docking to the $GABA_AR$. With the $GABA_AR$ model and anesthetic ligand docking validation derived from our previous work (1, 2), a set of in silico molecular docking calculations was developed using members of the series of known etomidate-like derivatives (6, 8). The most potent agent for $GABA_AR$ potentiation within this series is known as 1n or TG41 (8). However, since this compound contains an imidazole nitrogen as in etomidate that is known to inhibit 11CYPB, the enzyme critical for corticosteroid biosynthesis, we modified the structure of the most potent version of this series to a unique compound (referred to as carbo-1n in Fig. 1) in a manner similar to the conversion of etomidate to carboetomidate (9) by merely substituting the nitrogen with a carbon atom (4, 21, 22). This compound has never been synthesized to the best of our knowledge, as demonstrated by a lack of hits in a structure-based search of most large publicly available chemical structure databases. Since carbo-1n is not commercially available and the means for its synthesis were initially lacking, we searched the Chemical Abstracts database for other commercially available structures with at least 80% structural similarity to carbo-1n for purposes of in silico docking and possible future in vitro and in vivo testing. A much larger series of compounds with known $GABA_AR$ EC_{50}s was then compiled for docking so as to develop a more robust docking score correlation at our validated $GABA_AR$ binding locale as follows: 20 members of the initial 1n series, the series of 6 phenolic/propofol-like derivatives from our previous work, R-etomidate, and R-carboetomidate. Additionally, our series of compounds with similarity to carbo-1n (11 found via the aforementioned structural similarity search) and without known $GABA_AR$ potency were then added to the docking calculation as noted below to predict relative orders of potency and infer which would be best to submit for further in vitro and in vivo testing.

All subsequent docking calculations were carried out using the Discovery Studio 4.0 software suite (Biovia Inc., San Diego, CA). The receptor binding site within the heteromeric $GABA_AR$ into which our compound series could be docked was created by using the propofol docking site in the $GABA_AR$ from our previous work, and allowing residues within a 5-Å radius of the docked propofol to be flexible, while maintaining rigidity of the remainder of the protein using the formalized Flexible Docking algorithm within the Discovery Studio 4.0 software suite (23). Modification of this binding site, so as to allow for larger ligands than propofol, was created by allowing the most potent of the aforementioned derivatives from Mascia et al. (8, 20), 1n, to dock into its most favorable pose while relaxing the adjacent amino acid sidechains, thereby creating an induced-fit binding site which would presumably be most favorable to ion channel opening, given the great potency and relative rigidity of 1n.

Once obtained, further flexible docking was performed using the aforementioned etomidate-like derivatives within the series pertaining to 1n, the carbo-1n derivative itself, and finally 11 compounds with at least 80% similarity to carbo-1n (Fig. 2). The settings for this calculation also allowed for a 5-Å radius about the centroid of the binding pocket within which amino acid sidechains were allowed to move. The best score for each ligand pose was then correlated with the $GABA_AR$ potentiation EC_{50} for those compounds in the docked series where such data were available. Docking scores were further obtained for carbo-1n and its 11 similar compounds to determine predicted potencies and to guide further purchases of the compounds where available for implementation in subsequent experiments.

Molecular Modeling of the 11-β-Hydroxylase Enzyme and Its Interactions with Etomidate, Carboetomidate, 1n, and Carbo 1n. The amino acid sequence of the human 11CYPB was obtained from the National Center for Biotechnology Information database. A BLAST sequence search was performed using this sequence to search for sequences of high homology from those with known 3D structures. The 4 best-scored homologous human sequences were downloaded as 3D coordinates from the Research Collaboratory for Structural Biology (RCSB) database (24). A multiple structure alignment was performed via the SAlign algorithm (25) to create a sequence profile based upon this structural alignment. Similarly, a BLAST sequence search (26) was performed using the human 11CYPB sequence to search for sequences of high homology from all known amino acid sequences. A multiple sequence alignment was performed from the resulting 211 sequences identified with good homology using the ClustalW algorithm (27). A profile (from the multiple structure alignment) to profile (from the multiple sequence alignment) alignment was then performed with ClustalW so as to align the sequence of the unknown structure with those of the known structures. The Modeler module (28) was used for assignment of coordinates for aligned amino acids, the construction of possible loops, and the initial refinement of amino acid sidechains. Normal mode analysis was performed using the LAABEN elastic network algorithm (29). Partial atomic charges for the heme moiety were computed using a combined quantum mechanics–molecular mechanics single point calculation for the heme group region using DMol

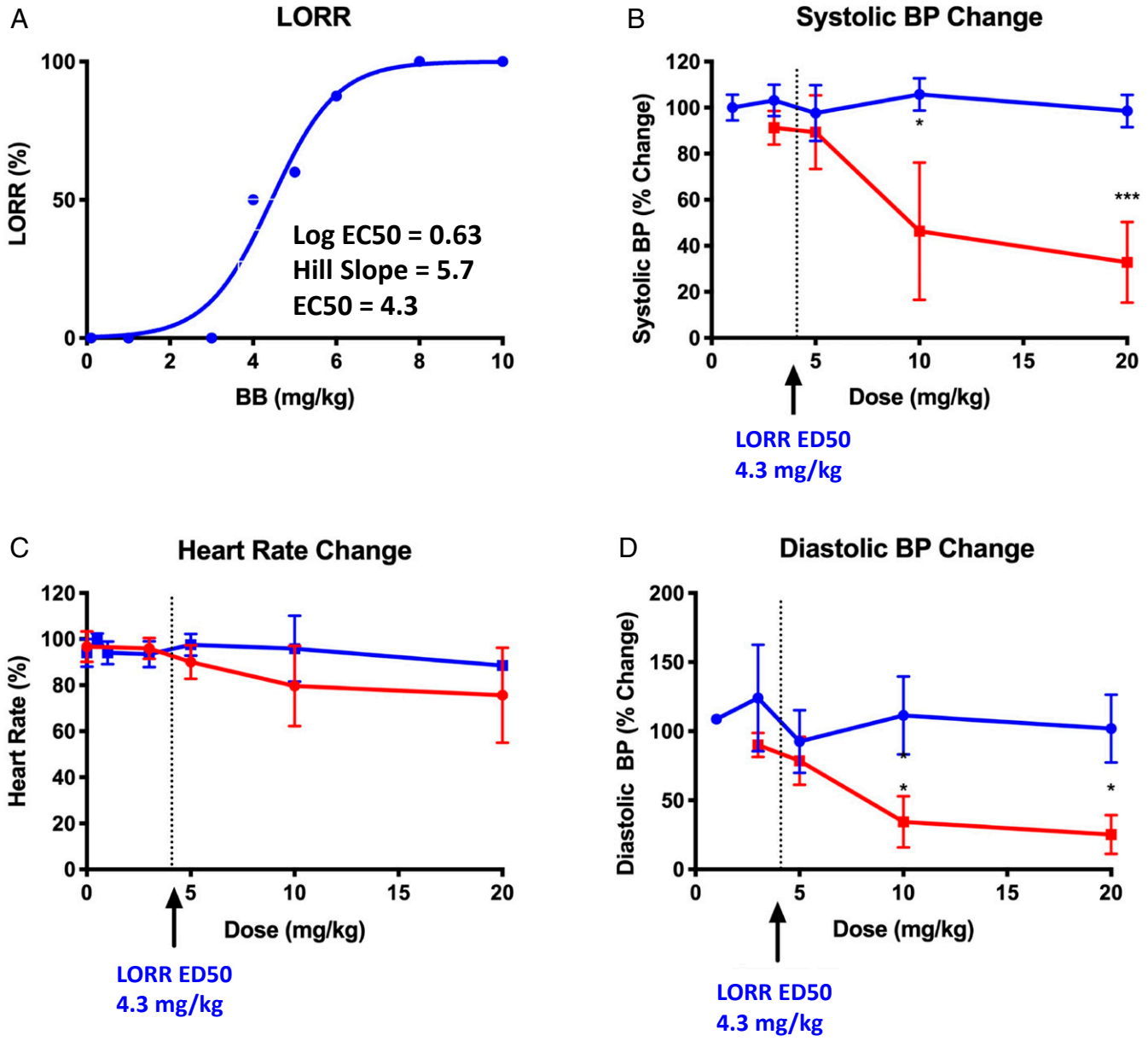

Fig. 7. (*A*) The dose–response curve for LORR in rats due to IV-administered BB (closed blue circles) showing anesthetic-induced LORR having an ED_{50} of 4.3 mg/kg. (*B*) BB had no effect on systolic blood pressure up to 20 mg/kg, whereas IV administration of propofol (closed red squares) significantly reduced systolic blood pressure ($n = 5$ $P < 0.01$) at 20 mg/kg; both have minimal effects on (*C*) heart rate. (*D*) The diastolic blood pressure was also suppressed compared with propofol ($n = 5$, $P < 0.05$ at both 10 mg/kg and 20 mg/kg). Error bars refer to SEs from the mean. The blood pressure and heart rates were recorded at 3 min after initiation of the drug injection.

density functional theory (30) and a Perdew–Burke–Ernzerhof functional, while the remainder of the complex was treated with a CHARMm molecular mechanics forcefield (31). Molecular dockings of etomidate and carboetomidate stereoisomers, as well as the 1n and carbo-1n compounds, were performed with the CDocker algorithm as noted above.

Loss-of-Righting Reflex in Tadpoles. Early prelimb-bud stage *Rana catesbeiana* tadpoles (5 per 50-mL beaker) were placed in room temperature oxygenated water buffered with 2.5 mM Tris·HCl buffer (pH = 7.4) and containing a concentration of test compound ranging from 0.1 μM to 100 μM. Tadpoles were manually tipped every 5 min with a steel spatula or stream of water and assessed for their ability to maintain righting reflex response until 120 min had elapsed. Tadpoles were deemed to have attained LORR if they failed to right themselves within 5 s after either spontaneous self-turning or being manually turned over on their back. At the end of each study, tadpoles were transferred to fresh water to assess whether the anesthetic action was reversible.

***Xenopus laevis* Oocyte Preparation and Electrophysiology.** For cDNA injections, stage 4 to 5 *Xenopus laevis* oocytes were purchased from Ecocyte (Dallas, TX). A Drummond Nanoject III was used to inject 40 nL of cDNA coding for α5, β3, and γ2 subunits in a 1:1:10 ratio, respectively, into each oocyte. Oocytes were stored in incubation medium (ND96 supplemented with 2 mM sodium pyruvate, 50 mg/mL gentamicin, and 10 mL of heat-inactivated HyClone horse serum [VWR, San Dimas, CA], adjusted to pH 7.5) in Petri dishes (VWR). All solutions were sterilized by passage through 0.22-μM filters. Injected oocytes were stored at 18 °C for 48 h, then used in electrophysiology experiments up to 1 wk after injection. All chemicals used were reagent grade and purchased from Sigma-Aldrich. GABA stock solutions were prepared from powder and diluted with modified Barth's solution (MBS) containing 88 mM NaCl, 1 mM KCl, 10 mM Hepes, 0.82 mM $MgSO_4$, 2.4 mM NaHCO3, 0.91 mM CaCl2, and 0.33 mM Ca(NO3)2, adjusted to pH 7.5 (17). BB stock solutions were prepared by dissolving powder forms with dimethyl sulfoxide (DMSO) and serially diluted with MBS (DMSO ≤ 0.05%)

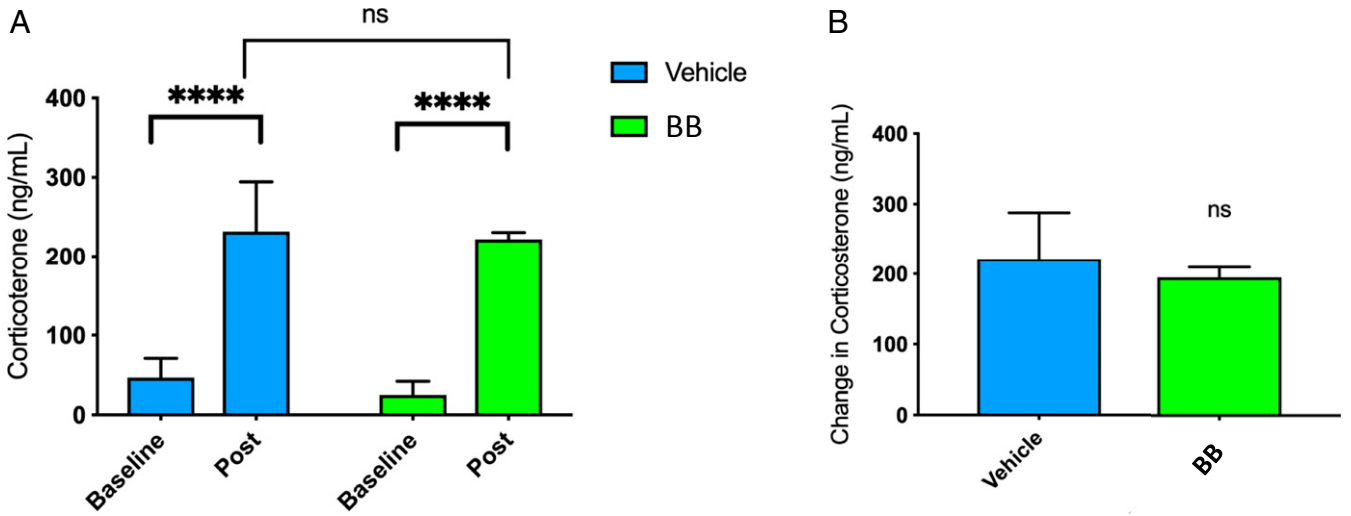

Fig. 8. (*A*) The effect of BB (10 mg/kg IV) given immediately after administering $ACTH_{1-24}$ (0.5 mg/kg IV) to cannulated rats previously treated 2 h prior with dexamethasone (0.5 mg/kg, IV). No difference in baseline levels before ACTH and compound administration were detected [$F(2, 17) = 1.13$, $P = 0.35$]. $ACTH_{1-24}$ along with either vehicle or KSEB caused robust corticosterone synthesis [$F(1,17) = 84.9$, $P = 0.0001$]; however there was no difference in corticosterone levels between posttreatment vehicle and BB [$F(1, 22) = 0.23$, $P = 0.64$]. (*B*) The effect of the vehicle or BB (10 mg/kg IV) on corticosterone synthesis expressed as a change in corticosterone levels shows no difference between the vehicle and BB effects [$F(2, 16) = 0.22$ $P = 0.80$]. Data are presented as mean ± SEM. ****, statistically significant differences; ns, no statistical difference.

immediately before testing. Pilot studies found that the DMSO present in solution, had no discernible effect on $\alpha5\beta3\gamma2$ $GABA_AR$ currents, in the presence or absence of agonist.

For the whole-cell recordings in oocytes, 2-electrode voltage-clamp recordings were performed according to previously reported techniques (32, 33). In brief, oocytes were clamped at a membrane potential of −70 mV using oocyte clamp OC-25C (Warner Instruments, Hamden, CT), and the oocyte recording chamber was continuously perfused with MBS ± drug and/or agonist (EC_{20} GABA) using a Dynamax peristaltic pump (Rainin Instrument Co., Emeryville, CA) at 3 mL/min using an 18-gauge polyethylene tube (Becton Dickinson, Sparks, MD), and resultant currents were recorded.

In Vitro Brain Slice Electrophysiology: Extracellular Recordings. Hippocampal brain slices were prepared from male Sprague-Dawley rats (Charles River Laboratories, Wilmington, MA) as described elsewhere (34). Briefly, rats were deeply anesthetized with isoflurane before decapitation. The brain was quickly removed and placed in ice-cold ACSF that was saturated with 95% O_2 and 5% CO_2 (carbogen) to achieve a pH of 7.4. Coronal brain slices were prepared using a vibratome (model VT1500, Leica) and 400-μm-thick slices were hemisected and placed on cellulose filter papers. They were stored at a gas (carbogen)–liquid ACSF interface in a holding chamber for at least 1 h before use. Single slices were transferred to a recording chamber and submerged in room temperature (22 °C) ACSF flowing at a rate of 3.0 mL/min. ACSF was saturated with carbogen by bubbling the solution for at least 15 min before use. Electrically evoked field potentials were measured using thin-walled glass pipettes (1.0 inner diameter, 1.5 outer diameter; Garner Glass Co., CA) filled with ACSF. Electrodes were placed in the stratum oriens, close to the CA1 cell body layer, to record population spikes. Bipolar tungsten microelectrodes (10 MOhm, Frederick Haer & Co., ME) were placed in stratum radiatum and used to stimulate Schaffer-collateral fibers to synaptically drive CA1 neurons. Responses were measured and plotted in real time to ensure that stable baselines (< 2.0% variation) were recorded for at least 20 min before experimental drug exposures began with BB (40 μM), propofol (10 μM), etomidate (4 μM), and control vehicles, picrotoxin (100 μM) or flumazenil (10 μM).

In Vitro Brain Slice Electrophysiology: Intracellular Recordings. Whole-cell electrophysiological recordings were carried out in hippocampal tissue prepared from C57/Black6 mice (P28 to P50; The Jackson Laboratory, Sacramento, CA). The 250-μm-thick transverse hippocampal slices were prepared with a similar method to the extracellular recordings, and described elsewhere (35). CA1 pyramidal cells (PCs) were patched under visualized guidance using infrared differential interference contrast microscopy at 60× magnification and recorded in whole-cell voltage-clamp mode. For recording all IPSCs, hippocampal slices were completely submerged and continuously superfused at a flow rate of 3 mL/min with ACSF containing NMDA and AMPA/Kainate receptor antagonists (25 μM d-APV and 10 μM NBQX). IPSCs were recorded at −70 mV with an internal solution containing (in mM): 130 $CsMeSO_3$, 10 Hepes, 0.4 EGTA, 6 TEA-Cl, 7 Na_2 phosphocreatine, 4 MgATP, 0.4 NaGTP, 0.1 spermine, 4 QX-314 Cl (pH 7.3; 290 to 295 mOsm). Series resistance (Rs, typically 10 to 20 MΩ) was continuously monitored throughout each experiment with a −5 mV, 80-ms command pulse delivered before each stimulus pair; cells with more than 10% change in Rs were excluded from analysis.

To evoke IPSCs, paired, monopolar square pulse stimuli (200-μs pulse width, 100-ms interval) were delivered through a stainless-steel electrode placed in the middle third of stratum radiatum. Stimulus intensity was adjusted to evoke IPSCs of comparable amplitudes across experiments (0.1 to 0.6 nA). IPSCs were monitored every 15 to 20 s. Once 5 min of stable IPSC amplitude was evoked (<15% variation), BB (40 μM) or vehicle, composed as previously described, was added to the perfused ACSF solution, and washed out after 10 min. IPSC amplitude, series resistance, input resistance, and holding current were monitored in real time during the experiment. Decay kinetics of IPSCs were measured offline as follows: a monoexponential function ($y = C0 + C1 \times \exp(-x/\tau)$) was fit to the region starting at the peak of the second IPSC and ending after the decay of the IPSC back to baseline. All timecourse data were obtained by measuring stated parameters for each pair of evoked IPSCs and averaging these values into 1-min bins. Time courses for both τ and evoked IPSC amplitude were normalized to their respective average values during the 5-min predrug baseline period. Postdrug measurements were made using averaged values taken between 10 and 15 min after drug application.

Anesthetic Potency of Test Compounds in Conscious Rodents. Three-month-old Sprague–Dawley male rats (Charles River Laboratories) were anesthetized with 3% isoflurane. Rodents were then instrumented with a catheter placed into the right internal jugular vein. The catheter was then sutured and s.c. tunneled to the posterior nape of the neck. Rats were then allowed to recover from anesthesia for 2 h. Following surgical recovery, rodents were tested with either BB or vehicle infused over 1 min via the jugular vein catheter. The effect of BB on activity level or sedative/anesthetic action as seen in LORR, in addition to the cardiovascular effects of the drug were monitored.

Hemodynamic Response of Test Compounds in Rodents. Three-month-old male Sprague–Dawley rats were obtained and anesthetized with thiobutabarbital sodium (Inactin, 100 mg/kg ip; Sigma, St. Louis, MO), a tracheotomy was performed, and the lungs were mechanically ventilated (model CV-101, Columbus Instruments, OH) at 38 to 45 breaths per minute using an air/oxygen mixture. Body temperatures were kept constant between 36.5 and 37.5 °C by use of a heating pad and by positioning surgical lamps placed over the heart. The left jugular vein was cannulated for administration of drugs.

The right common carotid artery was cannulated for measurement of blood pressure and heart rate via a PE23 pressure transducer. The transducer was connected to an ADInstruments (Colorado Springs, CO) quad bridge and blood pressure was monitored continuously throughout the duration of the experiment through LabChart version8 (ADInstruments). Heart rate and blood pressure were quantified for each of the study groups when either BB (2.5, 5, 10, and 20 mg/kg), BB vehicle (5% Pharmasolve, 30% PEG, 3% ethanol, and 62% solutol in 30% water, pH 8.0), or propofol (0, 2.5, 5, and 10 mg/kg) were infused IV over 1 min through the right internal jugular vein. The blood pressure and heart rate effects of a given dose were recorded 3 min after initiation of the drug injection.

Data Analysis. High-throughput screening was performed using the Flexible Docking and CDocker algorithms within Discovery Studio 4.0 (Accelrys Inc., San Diego, CA), as well as with the Chemical Abstracts database for the search of commercially available structures. All in vivo analyses where conducted using Prism 6.0 (GraphPad Software, Inc., San Diego CA); for each data point, 5 animals were tested. Dose–response curves were analyzed using the regression method adapted from Waud et al. (36). Electrophysiology recordings were analyzed with Igor Pro Software (Wavemetrics, Portland, OR). Each graph was the result of 5 experiments to report average response at each and SDs.

Corticosteroid Response of Test Compound in Rats. We used the methods of Wang et al. (18) to examine the interaction of BB with corticosterone synthesis, specifically its ability of test compounds to inhibit 0.5 mg/kg $ACTH_{1-24}$ (Sigma-Aldrich, St. Louis MO) stimulated synthesis. The jugular veins of Sprague–Dawley rats were cannulated under isoflurane anesthesia and allowed to recover. Dexamethasone (0.5 mg/kg) was administered 2 h before administration of 25 μg/kg IV $ACTH_{1-24}$ and the test compound. The dose of BB administered was 10 mg/kg, slightly more than 2 times the ED_{50} for LORR. Blood samples were taken before ACTH and test compound administration and then 30 min after. Serum corticosterone levels were determined by ELISA kit for corticosterone (ALPCO).

ACKNOWLEDGMENTS. We acknowledge Professor James Trudell for his valuable and helpful comments, as well as Gabriella Bertaccini, Grace Ramey, Dr. Peyman Sahbaie, Lawrence Fu, and Timothy Li for their technical assistance. This work was supported by NIH Grants GM119522 (to E.R.G.) and MH110610 (to B.D.H.); the Department of Anesthesiology, Perioperative, and Pain Medicine at Stanford University; the Office of Technology and Licensing at Stanford University; and the US Department of Veterans Affairs. Further, this material is the result of work supported with resources and the use of facilities at the Palo Alto VA Health Care System, Palo Alto Division. Finally, we would like to extend our sincere thanks to Dr. Mehrdad Shamloo and Rachel K. Lam within the Stanford Behavioral and Functional Neuroscience Core Laboratory (BFNL) for their help with adrenal corticosteroid assays.

1. E. J. Bertaccini, O. Yoluk, E. R. Lindahl, J. R. Trudell, Assessment of homology templates and an anesthetic binding site within the γ-aminobutyric acid receptor. *Anesthesiology* **119**, 1087–1095 (2013).
2. V. S. Fahrenbach, E. J. Bertaccini, Insights into receptor-based anesthetic pharmacophores and anesthetic-protein interactions. *Methods Enzymol.* **602**, 77–95 (2018).
3. A. Jenkins *et al*., Evidence for a common binding cavity for three general anesthetics within the GABAA receptor. *J. Neurosci.* **21**, RC136 (2001).
4. S. A. Forman, Clinical and molecular pharmacology of etomidate. *Anesthesiology* **114**, 695–707 (2011).
5. R. L. Wagner, P. F. White, P. B. Kan, M. H. Rosenthal, D. Feldman, Inhibition of adrenal steroidogenesis by the anesthetic etomidate. *N. Engl. J. Med.* **310**, 1415–1421 (1984).
6. B. Asproni *et al*., Synthesis, structure-activity relationships at the GABA(A) receptor in rat brain, and differential electrophysiological profile at the recombinant human GABA(A) receptor of a series of substituted 1,2-diphenylimidazoles. *J. Med. Chem.* **48**, 2638–2645 (2005).
7. J. F. Cotten *et al*., Carboetomidate: A pyrrole analog of etomidate designed not to suppress adrenocortical function. *Anesthesiology* **112**, 637–644 (2010).
8. M. P. Mascia *et al*., Ethyl 2-(4-bromophenyl)-1-(2,4-dichlorophenyl)-1H-4-imidazolecarboxylate is a novel positive modulator of GABAA receptors. *Eur. J. Pharmacol.* **516**, 204–211 (2005).
9. S. Shanmugasundararaj *et al*., Carboetomidate: An analog of etomidate that interacts weakly with 11β-hydroxylase. *Anesth. Analg.* **116**, 1249–1256 (2013).
10. P. J. Lein, C. D. Barnhart, I. N. Pessah, Acute hippocampal slice preparation and hippocampal slice cultures. *Methods Mol. Biol.* **758**, 115–134 (2011).
11. M. C. Bieda, H. Su, M. B. Maciver, Anesthetics discriminate between tonic and phasic γ-aminobutyric acid receptors on hippocampal CA1 neurons. *Anesth. Analg.* **108**, 484–490 (2009).
12. M. B. MacIver, Anesthetic agent-specific effects on synaptic inhibition. *Anesth. Analg.* **119**, 558–569 (2014).
13. J. A. Gredell, P. A. Turnquist, M. B. Maciver, R. A. Pearce, Determination of diffusion and partition coefficients of propofol in rat brain tissue: Implications for studies of drug action in vitro. *Br. J. Anaesth.* **93**, 810–817 (2004).
14. R. A. Pearce, Physiological evidence for two distinct GABAA responses in rat hippocampus. *Neuron* **10**, 189–200 (1993).
15. M. Vargas-Caballero, L. J. Martin, M. W. Salter, B. A. Orser, O. Paulsen, alpha5 subunit-containing GABA(A) receptors mediate a slowly decaying inhibitory synaptic current in CA1 pyramidal neurons following Schaffer collateral activation. *Neuropharmacology* **58**, 668–675 (2010).
16. R. P. Bonin, L. J. Martin, J. F. MacDonald, B. A. Orser, Alpha5GABAA receptors regulate the intrinsic excitability of mouse hippocampal pyramidal neurons. *J. Neurophysiol.* **98**, 2244–2254 (2007).
17. H. T. Nguyen *et al*., Behavior and cellular evidence for propofol-induced hypnosis involving brain glycine receptors. *Anesthesiology* **110**, 326–332 (2009).
18. B. Wang *et al*., An etomidate analogue with less adrenocortical suppression, stable hemodynamics, and improved behavioral recovery in rats. *Anesth. Analg.* **125**, 442–450 (2017).
19. F. de Wit *et al*., The effect of propofol on haemodynamics: Cardiac output, venous return, mean systemic filling pressure, and vascular resistances. *Br. J. Anaesth.* **116**, 784–789 (2016).
20. M. P. Mascia *et al*., Differential modulation of GABA(A) receptor function by aryl pyrazoles. *Eur. J. Pharmacol.* **733**, 1–6 (2014).
21. S. A. Forman, Molecular approaches to improving general anesthetics. *Anesthesiol. Clin.* **28**, 761–771 (2010).
22. D. E. Raines, The pharmacology of etomidate and etomidate derivatives. *Int. Anesthesiol. Clin.* **53**, 63–75 (2015).
23. J. Koska *et al*., Fully automated molecular mechanics based induced fit protein-ligand docking method. *J. Chem. Inf. Model.* **48**, 1965–1973 (2008).
24. H. M. Berman *et al*., The protein data bank. *Nucleic Acids Res.* **28**, 235–242 (2000).
25. H. Braberg *et al*., SALIGN: A web server for alignment of multiple protein sequences and structures. *Bioinformatics* **28**, 2072–2073 (2012).
26. S. F. Altschul *et al*., Gapped BLAST and PSI-BLAST: A new generation of protein database search programs. *Nucleic Acids Res.* **25**, 3389–3402 (1997).
27. D. G. Higgins, J. D. Thompson, T. J. Gibson, Using CLUSTAL for multiple sequence alignments. *Methods Enzymol.* **266**, 383–402 (1996).
28. N. Eswar, D. Eramian, B. Webb, M. Y. Shen, A. Sali, Protein structure modeling with MODELLER. *Methods Mol. Biol.* **426**, 145–159 (2008).
29. E. J. Bertaccini, J. R. Trudell, E. Lindahl, Normal-mode analysis of the glycine alpha1 receptor by three separate methods. *J. Chem. Inf. Model.* **47**, 1572–1579 (2007).
30. B. Delley, Dmol, a standard tool for density functional calculations: Review and advances. *Theor. Comput. Chem.* **2**, 221–254 (1995).
31. B. R. Brooks *et al*., CHARMM: The biomolecular simulation program. *J. Comput. Chem.* **30**, 1545–1614 (2009).
32. A. Naito *et al*., Glycine and GABA(A) ultra-sensitive ethanol receptors as novel tools for alcohol and brain research. *Mol. Pharmacol.* **86**, 635–646 (2014).
33. D. I. Perkins *et al*., Loop 2 structure in glycine and GABA(A) receptors plays a key role in determining ethanol sensitivity. *J. Biol. Chem.* **284**, 27304–27314 (2009).
34. B. A. Dagne *et al*., High dose gamma radiation selectively reduces GABAA-slow inhibition. *Cureus* **9**, e1076 (2017).
35. P. Hoerbelt, B. D. Heifets, "Native system and cultured cell electrophysiology for investigating anesthetic mechanisms" in *Methods in Enzymology*, R. G. Eckenhoff, I. J. Dmochowski, Eds. (Academic Press, 2018), pp. 301–338.
36. D. R. Waud, On biological assays involving quantal responses. *J. Pharmacol. Exp. Ther.* **183**, 577–607 (1972).